

## EFFECT OF PORE SHAPE AND SIZE ON ENERGY ABSORPTION IN CELLULAR AL-SI12 MANUFACTURED BY INFILTRATION PROCESS

---

*Luis Edgar Moreno*

National University of Colombia –  
Manizales Campus – Faculty of Engineering  
and Architecture – Department of  
Industrial Engineering – Processing  
and Characterization of Materials for  
Engineering Research group – Advanced  
Metallic Materials Laboratory – Manizales –  
Colombia

*Sandro Báeza*

National University of Colombia –  
Manizales Campus – Faculty of Engineering  
and Architecture – Department of  
Industrial Engineering – Processing  
and Characterization of Materials for  
Engineering Research group – Advanced  
Metallic Materials Laboratory – Manizales –  
Colombia

All content in this magazine is  
licensed under a Creative Com-  
mons Attribution License. Attri-  
bution-Non-Commercial-Non-  
Derivatives 4.0 International (CC  
BY-NC-ND 4.0).



**Abstract:** The energy absorption capacity of irregular pore and rounded pore cellular metals with five pore sizes, subjected to quasi-static compression, was evaluated in this research. An aluminum-silicon alloy as base metal and sea salt particles as removable filler were used. The cellular metals were manufactured using a modified removable filler infiltration technique, in which a controlled atmosphere device that allows melting and infiltration of the metal in a single heating operation was used. Properties such as density, relative density, and porosity of cellular metals were obtained based on mass, volume, and simple equations involving these parameters. Stress-strain curves from the quasi-static compression tests were graphed and by integrating the area under their curve, the energy absorption capacity per unit volume was calculated. The results indicate that cellular metals with irregular pores have higher density, higher relative density and lower porosity, and in addition, greater energy absorption capacity compared to those with rounded pores. The scatter diagrams indicate a negative correlation between energy absorption capacity and pore size for the two pore shapes. The analysis of variance allows concluding that the energy absorption capacity is affected by the shape and size of the pore and by the interaction between these two parameters.

**Keywords.** cellular metals, infiltration process, quasi-static compression, energy absorption, pore size, pore shape.

## INTRODUCTION

Cellular metals or metallic foams are a relatively new class of materials that exhibit a particular combination of properties that cannot be obtained with any dense metal or any other bulk material [1]. They have high stiffness and specific resistance, excellent impact energy absorption, and outstanding damping and acoustic absorption properties [2]. The properties depend on the porous structure (shape, size, orientation and distribution of the pores) and the metal matrix [3]. Different metals such as magnesium, copper, titanium, aluminum and their alloys have been used as matrix in the manufacture of cellular metals. However, aluminum and its alloys are the most used due to their remarkable properties such as good ductility, low melting temperature, low density and high corrosion resistance [4].

A wide variety of techniques are currently used for the manufacture of cellular metals [5-10], which are usually classified according to different criteria. Depending on the state or stage of the matrix material [5,10], they are classified into metal melt techniques, solid metal powder techniques, and gaseous deposition techniques. According to cell topology, they are usually classified into techniques for manufacturing closed-pore cellular metals or metal foams and techniques for manufacturing open-pore cellular metals or metal sponges [8]. One of the most used techniques to obtain open-pore aluminum-based metals and their alloys is the infiltration of removable fillers, which is developed in five stages: 1. Molding of the “preform”; 2. Sintering of the “preform”; 3. Melting of metal; 4. Infiltration of the metal inside the preform, and 5. Dissolution of “preform” material [5,6,11]. With this technique, good quality cellular metals can be obtained, with very small pore sizes and their processing costs are not high [12,13]. However, it is a

slow process due to the number of stages and the duration of dissolution of the removable filler [6]. In search of more efficient processes, with fewer stages and lower costs, some modifications to this technique have been proposed [14,15,16]. One of them proposes using a device with a controlled atmosphere independent of the furnace in order to carry out the fusion and infiltration of the metal in a single operation. This modification allows the exact amount of metal to be injected into the removable filler, avoiding possible material waste and minimizing the oxidation of the liquid metal [17].

Probably the most notable mechanical property of cellular metals is their ability to absorb energy when subjected to compressive or impact forces. Thanks to this property, these materials can be used as energy absorbers or as almost ideal shock absorbers in the automotive, aeronautical, naval and railway industries, among others [8,18-20]. Based on the above, various studies in which the effect of different parameters on the energy absorption capacity under quasi-static compression of cellular metals has been published. Hassani et al [21], successfully manufactured open-cell aluminum foams with graded cell size and graded density through the dissolution sintering technique using spherical granulated carbamide as space support. The authors studied the compressive properties, including energy absorption of graded foams, comparing them with their non-graded counterparts. The results showed that the foams graded by cell size absorbed more energy than those of not graded similar foams because they showed a wider plateau region and greater densification strain in the stress-strain curve Bafti and Habibolhazadeh [2], researched the effects of the shape and size of the cells and the relative density of aluminum foams on the ability to absorb energy by compression in aluminum foams produced by the dissolution

sintering technique. The results show that angular cells significantly reduce energy absorption. They also indicate that energy absorption increases with cell size and the relative density of the foams. Kadkhodapour et al [22] used experimental procedures and numerical methods to evaluate the effect of regular and irregular pore distribution, as well as load direction on the compression properties of aluminum foams with hollow spheres. The results of compression tests showed that for irregular samples the energy absorption capacity in high deformations was reduced due to non-uniform deformation compared to regular foams. Fateme and Paydar [18], manufactured aluminum foams with different pore structures, some with uniform structure and others with gradient through powder metallurgy using carbamide as a space support. The results showed that density gradient foams exhibit higher energy absorption capacity than uniformly structured foams of the same relative density.

The purpose of this research was to fabricate cellular metals with two different shapes and five pore sizes in order to determine and compare properties such as density, relative density, porosity and energy absorption capacity under quasi-static compression, and to evaluate the effect of shape and pore size on energy absorption capacity. For the fabrication of cellular metals, a modified removable filler infiltration technique was used, using an aluminum-silicon alloy as a matrix and irregularly shaped and rounded sea salt particles as removable fillers to generate the pores.

## EXPERIMENTAL PROCEDURES

### MATERIALS

The metal material used as a matrix in this research was the aluminum-silicon alloy commonly referred to as Al-Si12. The alloy, in the form of ingots, is produced by the Colombian company Propulsora S.A and according to this supplier the chemical composition is 85.5% Al, 12%Si, 0.8% Fe and 2.2% other elements. The melting temperature is in the range of 650- 750°C and the density is 2.66 g/cm<sup>3</sup>. Sea salt with a purity of 99% NaCl, melting point of 801°C and density of 2.17 g/cm<sup>3</sup> was used as a removable filler. This material is produced by the Colombian company Aquasal.

The salt was classified by size using a Pinzuar brand electric sieve. Table 1 shows the identification of the five particle sizes used, which shall be the same for the pore size, the sieve number and the size range in millimeters.

Particle/pore size identification	Sieve number	Size range (mm)
T1	4 - 5	4,0 - 4,75
T2	¼ - 4	4,75 - 6,3
T3	5/16 - ¼	6,3 - 8,0
T4	3/8 - 5/16	8,0 - 9,5
T5	7/16 - 3/8	9,5 - 11,2

**Table 1** Identification of particle/pore size, sieve number and size range.

### PARTICLE ROUNDING

To carry out the rounding of the particles, a special equipment was designed and built, which is in the process of being patented. In general terms, the equipment consists of an electric motor that transmits rotational movement through a system of pulleys and belts to an axis mounted on a chassis that houses two other parallel axes. On the axes are placed two cylindrical drums coated

internally with sandpaper whose grain size depends on the size of the salt particle to be rounded. The irregularly shaped salt particles are placed inside the drums in such a way that, due to the rotation and friction of the particles with the sandpaper and between themselves, they acquire the rounded shape. Once the process is finished, they are classified by size in the electric sieve.

### OBTAINING CELLULAR AL-SI12

Cellular metals based on Al-Si12, irregular pore and rounded pore, were manufactured using a modified removable filler infiltration technique, which uses a controlled atmosphere device for metal fusion and infiltration processes in a single heating operation. The function of the device is to allow the manufacture of porous metals from metals or alloys whose melting temperature is less than 750°C, through the infiltration of removable fillers using conventional furnaces [17]. The device consists of a vacuum chamber with an internal thread at the top in which a threaded ring is located to fix the mold-container system. In addition, it is equipped with a cooling coil to protect the Orings. The other component is the hermetic sealing cap which consists of a four-way adapter to which two regulating valves are attached, one connected to the vacuum pump and the other connected to the inert gas tank, and a manovacuumeter for pressure control inside the device. Fig. 1 shows the device with its components. This technique is carried out in four stages, which can be consulted in Báez et al [11].

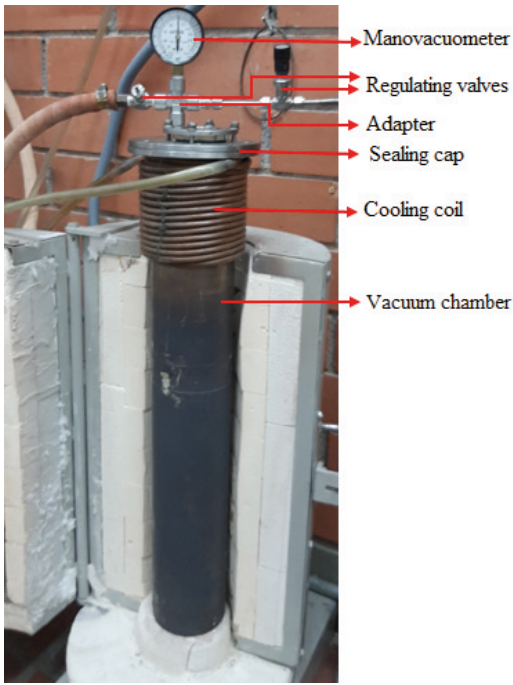


**Fig. 1** Controlled atmosphere device with its main parts. Source: author.

### QUASI-STATIC COMPRESSION TEST

The quasi-static compression test was carried out on a Humbolt Master Loader digital machine, with a load capacity of 50 kN. For each shape and pore size, five cylindrical specimens of 42 mm diameter and 34 mm height were tested at a speed of 2 mm/minute, corresponding to a strain rate of  $9.8 \times 10^{-4} \text{ s}^{-1}$ . Unit stress and strain values were calculated by relating the force to the area of each specimen and the strain to their height. Unit stress-strain curves were plotted and values corresponding to plateau stress and densification strain, from each plot were obtained. The plateau stress ( $\sigma_{pl}$ ) was calculated by taking deformations of 20% and 40% and averaging their respective stress according to the recommendation of ISO 13314:2011[23]. Densification deformation ( $\epsilon_d$ ) was determined by the energy absorption efficiency method [24]. The energy absorption capacity of each test piece was obtained with the support of software by integrating the area under the curve for deformations between 0 and the densification deformation.

## RESULTS AND DISCUSSION

### ROUNDING OF PARTICLES AND DETERMINATION OF STRUCTURAL CHARACTERISTICS

Irregularly shaped T8-sized particles are shown in Fig. 2a and rounded particles of the same size are shown in Fig. 2b.



Figure 2. a) Irregular particles size T8 and b) Rounded particles size T8.

Based on equations 1, 2 and 3, values were obtained for the density, relative density and percentage of porosity of cellular metals with irregular pore and rounded pore. Average values with their standard deviation can be found in Table 2.

$$\delta_{m.c} = \frac{m_{m.c}}{v_{m.c}} \quad (1)$$

$$\delta_r = \frac{\delta_{m.c}}{\delta_m} \quad (2)$$

$$\%P = (1 - \delta_r) * 100 \quad (3)$$

In equations 1, 2 and 3:  $\delta_{m.c}$  (cellular metal density),  $m_{m.c}$  (cellular metal mass),  $v_{m.c}$  (cellular metal volume),  $\delta_r$  (relative density),  $\delta_m$  (matrix density or base metal) and  $\%P$  (percentage porosity of cellular metal).

Table 2 shows that the average density and relative density of irregular pore cellular metals for all sizes is higher than that of rounded pore and the average porosity percentage is lower. Rounding of the particles resulted in an average decrease of 22.8% in density and relative density and an increase in porosity of 10.1%. This result is logical considering that, for a constant volume of the mold, it was necessary to use less quantity (mass) of salt and more metal in the manufacture of irregular pore samples for every one of the five sizes, which translates into higher density and higher relative density. However, due to their shape, the rounded particles registered greater packing inside the mold, which means greater mass. Therefore, after the dissolution process, they generated more space which resulted in greater porosity.

## RESULTS OF MECHANICAL CHARACTERIZATION

Stress-strain curves under quasi-static compression for five pore sizes of cellular Al-Si12 with irregular pore (I) and rounded pore (R), are shown in Fig. 3.

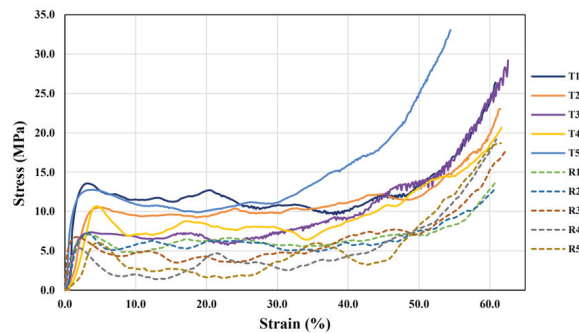


Fig. 3 Stress-strain curves of Al-Si12 with irregular pore and rounded pore, for five pore sizes.

In the curves of Fig. 3, three regions can be identified that are typical in cellular metals subjected to compression. A short elastic initial region in which the stress is directly proportional to the strain unit, a second plastic region, called the plateau region, characterized by significant increase in unit strain keeping the stress almost constant, and a third region in which the stress is increased without a significant increase in the unit strain, which corresponds to the densification region [10,18,25-27].

After applying the methodologies to obtain plateau stress, densification deformation and energy absorption capacity stated above, average values and standard deviation of these properties were calculated, which are presented in Table 3.

Based on the average values of energy absorption capacity, dispersion diagrams were designed according to the pore size, which are presented in Fig. 4.

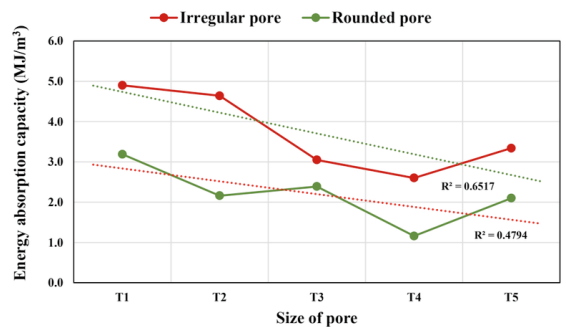


Fig. 4 Dispersion diagrams of energy absorption capacity with respect to the pore size of cell Al-Si12 with irregular pore and rounded pore.

The scatter diagrams show that there is a negative correlation between the energy absorption capacity and the pore size for the cellular metals obtained, both with irregular pores and rounded pores. For those with irregular pores the correlation is high given the correlation coefficient (0.80), while for those with rounded pores the correlation

Pore size	Irregular pore			Rounded pore		
	Density (g/cm <sup>3</sup> )	Relative density (%)	Porosity (%)	Density (g/cm <sup>3</sup> )	Relative density (%)	Porosity (%)
T1	0,92 ± 0,07	34,51 ± 2,49	65,49 ± 2,49	0,78 ± 0,05	29,45 ± 1,73	70,55 ± 1,73
T2	0,95 ± 0,01	35,79 ± 0,49	64,21 ± 0,49	0,73 ± 0,03	27,43 ± 1,23	72,57 ± 1,23
T3	0,91 ± 0,03	34,36 ± 0,98	65,64 ± 0,98	0,79 ± 0,05	29,67 ± 1,77	70,33 ± 1,77
T4	0,94 ± 0,06	35,19 ± 2,40	64,81 ± 2,40	0,73 ± 0,06	27,49 ± 2,13	72,51 ± 2,13
T5	0,96 ± 0,02	36,17 ± 0,82	63,83 ± 0,82	0,78 ± 0,08	29,15 ± 2,96	70,85 ± 2,96

**Table 2** Average values and their standard deviation of the density, relative density and porosity of Al-Si12 with irregular pore and rounded pore.

Pore size	Irregular Pore			Rounded Pore		
	Plateau stress (MPa)	Densification strain (%)	Energy absorption (MJ/m <sup>3</sup> )	Plateau stress (MPa)	Densification strain (%)	Energy absorption (MJ/m <sup>3</sup> )
T1	10,45 ± 1,95	49,26 ± 6,14	4,90 ± 0,56	6,63 ± 0,30	49,25 ± 4,55	3,19 ± 0,33
T2	9,05 ± 0,94	52,04 ± 3,53	4,64 ± 0,63	5,08 ± 0,65	43,28 ± 3,48	2,16 ± 0,43
T3	7,36 ± 1,85	45,09 ± 4,99	3,05 ± 0,98	5,65 ± 0,94	45,24 ± 3,94	2,39 ± 0,47
T4	7,62 ± 0,94	40,44 ± 4,24	2,60 ± 0,26	4,31 ± 1,29	31,78 ± 7,89	1,16 ± 0,38
T5	9,62 ± 2,30	39,84 ± 3,62	3,34 ± 0,38	5,06 ± 2,30	31,43 ± 9,29	2,1 ± 0,62

**Table 3** Average values and standard deviation of plateau stress, densification strain and Al-Si12 energy absorption capacity of irregular pore and rounded pore.

is moderate according to the correlation coefficient (0.69). The observed trend in the decrease of the energy absorption capacity as the size increases for the two pore shapes evaluated is due to the fact that both the plateau stress and the densification strain also tend to decrease as the pore size increases, as observed in Table 3, that is, there is a direct relationship between these two variables and the energy absorption, which is consistent with what has been proposed by several authors [24,25,28]. Results similar to those obtained here were reported by Hajizadeh et al [4] and Xia et al [29]. However, works with contrary results have also been reported. Ziad et al [27], manufactured cellular metals by the infiltration technique with two pore sizes, 2 and 4 mm, and concluded that the larger the pore size, the greater the energy absorption capacity. Regarding this work, there are important differences that make comparison difficult. For example, the salt particles used as removable filler were subjected to compaction

before infiltration, varying the pressure between 0.5 and 10 MPa and only worked with two pore sizes. Another research with contrary results is the one reported by Soni and Biswas [30]. It is also difficult to establish comparisons given the existing differences. The authors mentioned used an aluminum-magnesium alloy, the infiltration process was carried out with continuous pressure and the particle/pore sizes were smaller than those used in this research.

The Fig. 4 also shows that the energy absorption capacity in cellular metals with irregular pores is greater for each and every one of the pore sizes with respect to cellular metals with rounded pores, and this difference corresponds to 68.6%. This behavior can be explained from different points of view. First, one of the reasons for the higher energy absorption capacity of irregular pore cellular metals lies in their higher relative density, as mentioned previously when analyzing the values in table 2. This result coincides with the

result obtained in experimental studies carried out by several researchers in which they have concluded that the energy absorption capacity increases with the increase of the relative density or, what is the same, decreases with increased porosity [2,18,31,32]. Another explanation that supports the behavior described is that the energy absorption capacity depends directly on the plateau stress and the densification strain [23,29,30]. If Table 3, which summarizes the average values of these two properties for the two pore shapes is analyzed, it is evident that for each and every size of the irregular shape, both the plateau stress and the strain densification are higher. Furthermore, if the variations of the arithmetic averages of the two parameters are compared, the plateau stress has a greater impact on the energy absorption capacity, with a variation of 65%, while the variation of the densification strain is only 12.8%.

In order to give statistical support to the results described above, an analysis of variance of two factors was carried out: that is, the energy absorption capacity as a function of the size and shape of the pore, and the possible interaction between the two factors with a significance level of 0.05. After verifying that the data present a normal distribution and that the variances are homogeneous, and posing the null and alternative hypotheses for each factor and for the interaction between the two factors, the results obtained, using SPSS, are shown in Table 4.

Since the calculated significance level is lower than the established significance level, in all three cases the null hypothesis is rejected and the alternative hypothesis is accepted. This allows establishing that between the two shapes and between the five pore sizes there are significant differences between the energy absorption averages and, in addition, that the interaction between the shape and the pore size exerts a significant influence on

the energy absorption capacity. When the alternative hypothesis is accepted, it is relevant to apply a Tukey test to know in which factors the significant differences occur. However, this test is applicable to more than two factors and, therefore, it was applied for pore size. The results are summarized in Table 5.

Table 5 shows that cellular Al-Si<sub>12</sub> with pore size T1 (4-4,75 mm), has the highest average energy absorption capacity of the means corresponding to the two pore shapes. Shows there are no significant differences between the averages of the energy capacity absorption of the two pore shapes, corresponding to sizes T1 and T2. There are also no significant differences between the averages of the means between sizes T2 and T3, between sizes T3 and T5 and between sizes T4 and T5, with size T4 being the one with the lowest mean among all sizes. This means that, compared to all irregular pore and rounded pore sizes, the best option for an application where the requirement is compressive energy absorption capacity, would be the T1 size and, in particular, the irregularly shaped one because it does not require any transformation process as it happens with the rounded pore.

A work with some similarity to the one carried out here was published by Bafti and Habibolahzadeh [2]. The authors produced cellular metals by the dissolution sintering process by mixing aluminum powders, in different proportions, with spherical and angular carbamide particles of five different sizes. Using a quasi-static compression test, they determined the energy absorption capacity of the materials obtained. When comparing the results, they found that cellular metals with angular pores absorbed less energy than those with spherical pores due to a high concentration of stress in the matrix around angular pores and the heterogeneous distribution of the pores in the matrix. A similar behavior was expected



Energy absorption capacity (MJ/m <sup>3</sup> )					
Origin	Type III sum of squares	Degrees of freedom	Mean square	F	Calculated significance
Corrected model	68,600 <sup>a</sup>	9	7,622	26,132	0,000
Intersection	413,224	1	413,224	1416,702	0,000
Pore shape	34,478	1	34,478	118,206	<b>0,000</b>
Pore size	29,488	4	7,372	25,274	0,000
Interaction (shape * size)	4,634	4	1,159	3,972	<b>0,008</b>
Error	11,667	40	0,292		
Total	493,491	50			
Corrected total	80,267	49			

**Table 4** Results of the compression energy absorption capacity variance analysis for irregular pore and rounded pore of Al-Si12.

Energy absorption capacity (MJ/m <sup>3</sup> )					
HSD Tukey <sup>a,b</sup>					
Size of pore	N	Subset			
		1	2	3	4
<b>T4</b>	10	1,8800			
<b>T5</b>	10	2,3290	2,3290		
<b>T3</b>	10		2,7230	2,7230	
<b>T2</b>	10			3,4000	3,4000
<b>T1</b>	10				<b>4,0420</b>
Significance		0,356	0,487	0,057	0,079

**Table 5** Tukey test results applied to the different sizes of the two pore shapes.

in this work, but the result was the opposite since cellular metals with angular or irregular pores showed a greater energy absorption capacity compared to those with rounded pores. The difference in the results between the two works can be attributed to the fact that the mentioned authors controlled the relative density in such a way that it was similar by managing the proportions of the materials and the compaction of the mixture. On the contrary, in this project this property varied and therefore the plateau stress and the densification deformation varied, properties that directly affect the energy absorption capacity. The authors mentioned above also found that increasing the size of the spherical pore, the energy absorption capacity also increased. They explain this behavior by arguing that, with a larger particle size of

carbamide, the wall thickness, the length of the cell edges and the size of the nodes increase, also increasing the compression properties and of course the energy absorption capacity. In addition, the spherical shape of carbamide provides a homogeneous cell size and shape in the cellular metal and that materials with this type of structure show a uniform deformation behavior, similar to the behavior of foams or cellular metals with an ideal architecture. In this investigation, as the rounded pore size increased, the energy absorption capacity, on the contrary, decreased, possibly because the size and shape of the cells or pores are not homogeneous. In addition, as the pore size increases, the heterogeneity is greater and this directly affects the energy absorption capacity. The above indicates that the use of carbamide as a removable filler is more advantageous than

the use of rounded particles. In conclusion, the results of the two works compared are contradictory due to significant differences such as the technique used and the shape and sizes of the removable filler particles used.

## CONCLUSIONS

(1) Cellular metals based on the aluminum alloy Al-Si12 and sea salt as a removable filler of irregular pores and rounded pores with five different pore sizes were successfully manufactured by means of a modified removable filler infiltration process, using a controlled atmosphere device for the metal fusion and infiltration processes in a single heating operation.

(2) The stress-strain curves of irregular and rounded cellular Al-Si12 pores derived from the quasi-static compression tests are similar to those reported in the literature as typical curves for this type of materials, since clearly three regions can be identified in them: an initial elastic region, the plateau region and the densification region.

(3) The density and the average relative density of cellular metals with irregular pores for all sizes is 22.8% higher than that of those with rounded pores, because to obtain them it was necessary to use a greater mass of metal, which is translated into higher density and higher relative density. On the contrary, the average of porosity percentage is lower by 10.1%, because the salt mass was obtained using less empty space after dissolution and, of course, less porosity.

(4) Between energy absorption capacity and pore size, there is a high negative correlation in irregular pore cellular metals and a moderate negative correlation in rounded pore

cellular metals. In addition, the energy absorption capacity of irregular pore cellular metals is 68.6% higher than that of rounded pore cellular metals. This behavior is due to the fact that irregular pore cellular metals have higher relative density, higher plateau stress and higher densification deformation than rounded pore metals.

(5) Based on the analysis of variance of two-factors carried out, it is concluded that the energy absorption capacity of Al-Si12 base cellular metals, manufactured by the modified removable filler infiltration technique, is influenced by the pore shape, the pore size and the interaction between these two factors. In turn, cellular metals with pore size T1 (4.0-4.75 mm) presents the highest average energy absorption capacity of the averages corresponding to the two pore shapes.

(6) Irregularly shaped T1 pore-sized cellular metals would be the most suitable option to select for an application as an energy absorber because it is not only the material with the highest energy absorption capacity, but also because it does not require any transformation process as in the case of rounded pores, which minimizes time and costs.

## ACKNOWLEDGEMENTS

The authors would like to thank the National University of Colombia through VIE-DIMA-VI and FIA for financial support through HERMES projects numbers 54562, 59166, 57267 and 59031. In addition, they would like to thank the technical staff of the materials resistance laboratories.

## REFERENCES

- [1] SCHULER P, FISHER S, BÜHRIG-POLACZEK A, FLECK C. Deformation and failure behaviour of open-cell Al foams under quasistatic and impact loading [J]. *Materials Science & Engineering A*, 2013, 587: 250-261.
- [2] BAFTI H, HABIBOLAHZADEH A. Compressive properties of aluminum foam produced by powder-Carbamide spacer route [J]. *Materials and Design*, 2013, 52: 404-411.
- [3] OSORIO J, SUÁREZ M, LARA G, ALFONSO I, FIGUEROA I. Manufacturing of open-cell Mg foams by replication process and mechanical properties [J]. *Materials and Design*, 2014, 64: 136-141.
- [4] HAJIZADEH M, YAZDANI M, VESALI S, KHODARAHMI H, MOSTOFI TM. An experimental investigation into the quasi-static compression behavior of open-cell aluminum foams focusing on controlling the space holder particle size [J]. *Journal of Manufacturing Processes*, 2021, 70: 193-204.
- [5] BANHART J. Manufacture, characterisation and application of cellular metals and metals foams. *Progress in Materials Science* [J], 2001, 46: 559-632.
- [6] FERNÁNDEZ P, CRUZ LJ, COLETO J. Procesos de fabricación de metales celulares. Parte I: Procesos por vía líquida [J]. *Revista de metalurgia*, 2008, 44: 540-555.
- [7] FERNANDEZ P, CRUZ LJ, COLETO J. Procesos de fabricación de metales celulares. Parte II. Vía sólida, deposición de metales, otros procesos [J]. *Revista de Metalurgia*, 2009, 45: 124-142.
- [8] GARCIA MF. Commercial applications of metal foams: Their properties and production [J]. *Materials*, 2016, 9: 1-27.
- [9] SHWETA S, NARESH B. A survey of fabrication and application of metallic foams (1925–2017) [J]. *J Porous Mater*, 2018, 25: 537–554.
- [10] ALI N, SUSHILA R. Fabrication methods and property analysis of metal foams – a technical overview [J]. *Materials Science and Technology*, 2023, 1-27.
- [11] BÁEZ S, HERNÁNDEZ M, PALOMAR M. Processing and characterization of open-cell aluminum foams obtained through infiltration processes [J]. *Procedia Materials Science*, 2015, 9: 54-61.
- [12] SAN MARCHI C, MORTENSEN A. Deformation of open-cell aluminum foam [J]. *Acta materialia*, 2001, 49: 3959–3969.
- [13] CONDE Y, DESPOIS JF, GOODALL D, MARMOTTANT A, SALVO L, SAN MARHI C, MORTENSEN A. Replication Processing of Highly Porous Materials [J]. *Advanced Engineering materials*, 2006, 49: 794-803.
- [14] QUADRINI FA, ALBERTO BB, LUDOVICA RA, LOREDANA S. Replication casting of open-cell AlSi7Mg0.3 foams [J]. *Materials Letters*, 2011, 65: 2558–2561.
- [15] RAMIN JA, GHODRATOLLAH R. Producing replicated open-cell aluminum foams by a novel method of melt squeezing procedure [J]. *Materials Letters*, 2012, 76: 233–236.
- [16] BISWAS S, SONI B. Indian Patent, Application Number [P]. 742/DEL/2015.
- [17] BAEZ PS, HERNÁNDEZ RM, PALOMAR PM. 2013; México Patent [P]. MX2013008466A(B).
- [18] HASSANLI F, PAYDAR MH. Improvement in energy absorption properties of aluminum foams by designing pore-density distribution [J]. *Journal of Materials Research and Technology*, 2021, 14: 609-619.
- [19]. MOVAHEDI N, FIEDLER T, TASDEMIRCI A, MURCH GE, BELOVA IV, GÜDEN M. Impact loading of functionally graded metal syntactic foams. [J] *Materials Science & Engineering A*, 2022, 839: 1-11.

- [20]. YIN H, MENG F, ZHU L, WEN G. Optimization design of a novel hybrid hierarchical cellular structure for crashworthiness [J]. *Composite Structures*, 2023, 303: 1-27.
- [21] HASSANI, A HABIBOLAHZADEH, A, BAFTI H. Production of graded aluminum foams via powder space holder technique [J]. *Materials and Design*, (2012, 40: 510–515.
- [22] KADKHODAPOUR J, MONTAZERIAN H, SAMADI M, SCHMAUDER S, ABOUEI M. Plastic deformation and compressive mechanical properties of hollow sphere aluminum foams produced by space holder technique [J]. *Materials & Design*, 2015, 83: 352–362.
- [23] ISO 13314:2011 Standard. Mechanical Testing of Metals. Ductility Testing. Compression Test for porous and cellular metals, 2011.
- [24] LI Q, MAGKIRIADIS I, HARRIGAN J. Compressive strain at the onset of densification of cellular solids [J]. *Journal of cellular plastics*, 2006, 42: 371-390.
- [25] SUN Y, LI Q. Dynamic compressive behaviour of cellular materials: A review of phenomenon, mechanism and modelling [J]. *International Journal of Impact. Engineering*, 2018, 112: 74-115.
- [26] WAN Tan, LIU Yuan, ZHOU Can-xu, CHEN Xiang, LI Yanxiang. Fabrication, properties, and applications of open-cell aluminum foams: A review [J]. *Journal of Materials Science & Technology*, 2021, 62: 11-24.
- [27] ZIAD EZ, ABD-ALRAZZAQ AHMED M. Experimental investigation of infiltration casting process parameters to produce open-cell Al-A356 alloy foams for functional and mechanical applications [J]. *The International Journal of Advanced Manufacturing Technology*, 2022, 119: 6761–6774.
- [28] ASHBY MF, EVANS AG, FLECK NA, GIBSON LJ, HUTCHINSON JW, WADLEY HN [M]. *Metal foams: A design guide*. U.S.A: Planta Tree. 2000.
- [29] XIA Y, SHI J, MU Y. Compressive behaviour of open-cell Al–Si alloy foam produced by infiltration casting [J]. *Materials Science and Technology*, 2023, 39: 1-13.
- [30] SONI B, BISWAS S. Evaluation of mechanical properties under quasi-static compression of open-cell foams of 6061-T6 Al alloy fabricated by pressurized salt infiltration casting method [J]. *Materials Characterization*, 2017, 130: 198-203.
- [31] MICHAELIDIS N, STERGIODIA F, TSOUKNIDAS A, PAVLIDOU E. Compressive response of Al-foams produced via a powder sintering process based on a leachable space-holder material [J]. *Materials Science and Engineering A*, 2011, 528: 1662–1667.
- [32] WAN Tan, LIANG Gang-giang, WANG Zhao-ming, ZHOU Can-xu, LIU Yuan. Fabrication and compressive behavior of open-cell aluminum foams via infiltration casting using spherical CaCl<sub>2</sub> space-holders [J]. *Research & Development*, 2022, 19: 89-98.